ACS APPLIED MATERIALS & INTERFACES

Research Article

Cite This: ACS Appl. Mater. Interfaces 2018, 10, 26241−26247

www.acsami.org

# Light-Induced Interfacial Dynamics Dramatically Improve the Photocurrent in Dye-Sensitized Solar Cells: An Electrolyte Effect

Jiajia Gao,[†] Ahmed M. El-Zohry,[‡] Herri Trilaksana,[§] Erik Gabrielsson,[∥] Valentina Leandri,[†] Hanna Ellis,[‡] Luca D'Amario,[‡] Majid Safdari,[†] James M. Gardner,[†] Gunther Andersson,[§] and Lars Kloo*[,†]

[†]Division of Applied Physical Chemistry, Department of Chemistry, KTH Royal Institute of Technology, SE-100 44 Stockholm, Sweden

[‡]Department of Chemistry, Ångström Laboratory, Uppsala University, Box 523, SE-75120 Uppsala, Sweden

[§]Flinders Centre for NanoScale Science and Technology (CNST), Flinders University, Adelaide 5042, Australia

[∥]Dyenamo AB, Greenhouse Labs, Teknikringen 38A, SE-114 28 Stockholm, Sweden

Supporting Information

**ABSTRACT:** A significant increase in the photocurrent generation during light soaking for solar cells sensitized by the triphenylamine-based D−π−A organic dyes (PD2 and LEG1) and mediated by cobalt bipyridine redox complexes has been observed and investigated. The crucial role of the electrolyte has been identified in the performance improvement. Control experiments based on a pretreatment strategy reveals TBP as the origin. The increase in the current and IPCE has been interpreted by the interfacial charge-transfer kinetics studies. A slow component in the injection kinetics was exposed for this system. This change explains the increase in the electron lifetime and collection efficiency. Photoelectron spectroscopic measurements show energy shifts at the dye/$TiO_2$ interface, leading us to formulate a hypothesis with respect to an electrolyte-induced dye reorganization at the surface.

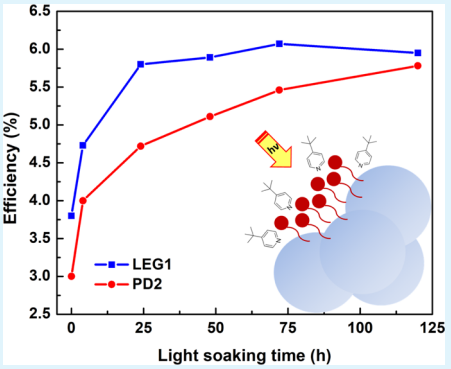


**KEYWORDS:** *dye-sensitized solar cells, electrolyte, interface, dynamics, light soaking*

## INTRODUCTION

Over the past two decades, the power conversion efficiency of dye-sensitized solar cells (DSSCs) has increased to over 13%.[1] Although the record efficiency is not impressive compared with other photovoltaic technologies, in particular with respect to perovskite-type hybrid solar cells, DSSCs still represent a perfect model for the fundamental study of charge-transfer dynamics, which can provide insights into structural and material engineering. The first and foremost step of charge transfer occurs at the dye/semiconductor interface in the kinetics ranging from femtosecond to millisecond. Photon absorption by the sensitizing dye molecules induces intramolecular charge separation followed by electron injection into the conduction band of the semiconductor. Therefore, a series of organic dyes with donor−π-linker−acceptor (D−π−A) configuration have been designed as sensitizer candidates for efficient intramolecular charge separation.[2−4] The design strategy of increasing the conjugation length of the linker unit has been widely exploited for broadening of the spectral absorption of the sensitizer and thus improving the photocurrent generation.[5−7] However, the engineering of the dye/$TiO_2$ interface with the aim to balance electron injection/recombination kinetics is highly critical but also quite difficult to monitor, as microscopic in situ interfacial characterization techniques are lacking.[8]

Interfacial properties of interest in DSSCs include binding mode and effective surface dipole moment of the adsorbed molecules.[9−11] Both properties will influence the interfacial electronic coupling and control the shift of the conduction band edge ($E_{CB}$) of the metal oxide substrate.[12−14] $E_{CB}$ defines the upper limit of the open-circuit voltage ($V_{oc}$) and affects the driving force of the dye/$TiO_2$ electron transfer; that is, the photocurrent is influenced as well. In light of this, molecular modification on metal oxides including dye sensitization is a common strategy to achieve an improvement of device performance. Furthermore, the anchoring configuration of dye molecules, which depends not only on the structure of the dye itself, but also on the effect of the local chemical environment, such as co-adsorbents or the electrolyte, is a primary factor to consider.[15,16] Other factors contributing to the interface structure involving surface treatment or interactions with electrolyte additives have to be considered as well. Cho et al. modified the $TiO_2$ surface with phosphonic acids before device assembly; the formed phosphonate dipole layer was shown to improve both the $V_{oc}$ and the short-circuit current ($J_{sc}$) through an upward shift of the $E_{CB}$.[10] A similar

Received: April 28, 2018
Accepted: July 11, 2018
Published: July 11, 2018






DOI: 10.1021/acsami.8b06897
ACS Appl. Mater. Interfaces 2018, 10, 26241−26247

effect has also been illustrated by Harima et al. regarding lithium intercalation in the $TiO_2$ substrate in DSSCs.[17] Dipolar molecules may also adjust the energetics at the interface by interacting with the dye layer instead. This strategy for promoting the DSSC performance has been applied by Buhbut et al. adding aromatic derivative co-solvents in the electrolyte.[9] Han's research group addressed shifts in energy levels of dye molecules and in the $E_{CB}$ of $TiO_2$ caused by the presence of potential-determining electrolyte additives, such as the commonly used 4-*tert*-butylpyridine (TBP) and lithium-ion-containing salts.[13] Molecular modification of the $TiO_2$ surface by forming a dipole layer, such as a chemisorbed monolayer, was reported to adjust the interface energetics and thus facilitate electron injection.[18,19]

In such an interactive system, the interfacial properties, especially at the photoanode/electrolyte interface, are actually variable as external conditions change. Photoinduced dye isomerization[20] and thermally induced dye degradation[21] essentially change the effective dipole moment on the $TiO_2$ surface. Under light or thermal stress, interactions involving the electrolyte with the dye/$TiO_2$ surface leading to interfacial energy level shifts and macroscopically performance variations have previously been documented.[22,23] However, the corresponding microscopic interactions, more likely involving the electrolyte components, have not been well identified and may limit our understanding of this interface chemistry. This work aims to provide some fundamental insights into the crucial effects of the electrolyte on a remarkable improvement of performance in a DSSC system.

Figure 1 shows the two representative organic dyes (LEG1 and PD2) selected for the present investigation, both

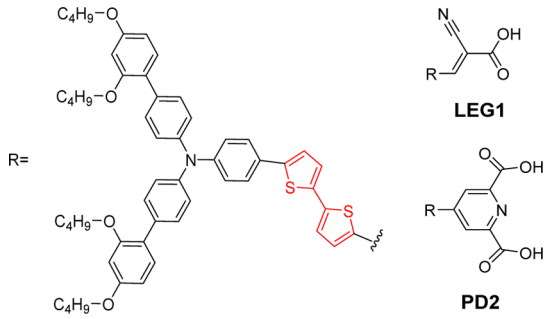


**Figure 1.** Chemical structures of the dyes LEG1 and PD2.

containing a D35-type donor (Figure S1) and a bithiophene group as $\pi$-linker but with two different anchoring groups. A preliminary study revealed that the performance of DSSCs sensitized by both dyes significantly improved upon exposure to light soaking conditions (full sun irradiation with 390 nm UV-cutoff filter and ~60 °C). Previous studies have demonstrated that the light absorption by the dye and the resulting photovoltaic performance of the assembled DSSCs were strongly influenced by the acidity of the electrolyte and the presence of pyridine additives.[24] Therefore, the investigation to rationalize the performance-improving phenomenon was focused on the electrolyte effect. According to the electrolyte composition, the electrolyte effects are separated into contributions of the Lewis base additive TBP and the redox-active cobalt complexes. Interfacial characterization measurements were combined in this work to interpret the underlying electrolyte effects from the perspectives of electron-transfer kinetics and dipole effects on the surface.

## RESULTS AND DISCUSSION

The dye PD2 contains a picolinic acid as an anchoring group with the intention to increase the dye binding strength to the $TiO_2$ substrate. In contrast, the dye LEG1 contains the commonly used cyanoacrylic acid anchoring group. Compared with the classic sensitizer D35 (the structure is shown in Figure S1) normally used for cobalt-polypyridine-mediated electrolytes, LEG1 contains a longer $\pi$-conjugated linker with one additional thiophene group resulting in a broader spectral absorption extending into the red region. Moreover, when exposing LEG1- and PD2-sensitized solar cells containing the optimized cobalt bipyridine electrolyte under open-circuit conditions to the light soaking for extended periods of time, the device efficiency significantly increase; see Figure 2, which

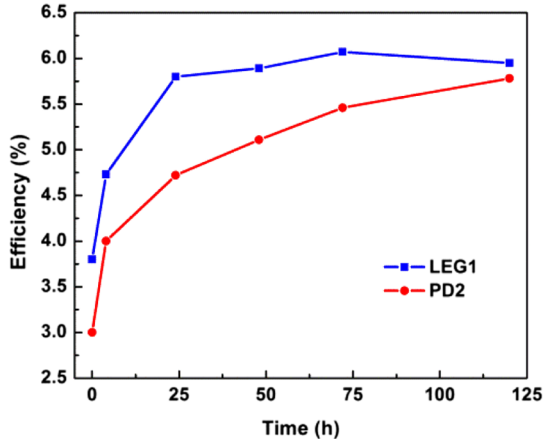


**Figure 2.** Evolution of DSSC power conversion efficiency vs time for the dyes PD2 (red, dots) and LEG1 (blue, squares) under continuous exposure to simulated solar light.

was not observed for D35-based devices. As shown in Figure S2, light of shorter wavelengths (<500 nm) plays a dominant role in the performance enhancement as compared to the effect of heat stress only. Components in the device sensitive to light in this wavelength range include the dye and cobalt complexes in the electrolyte. Compared with LEG1, the efficiency evolution of PD2-based DSSCs is larger and takes longer to reach a plateau value. Two possible reasons could be related: (1) the more robust anchoring group of PD2 with respect to LEG1 and (2) higher dye load on the $TiO_2$ surface for PD2, as reported in our previous work.[24] Therefore, an investigation focused on the dye molecular level and the dye/$TiO_2$ interface was undertaken to interpret the light-induced improvement of performance. The improvement is mainly manifested in the increase of photocurrent, as shown in Table 1. Consistently, the incident photon-to-current efficiency (IPCE) is increased as well, and in particular in the red region (Figure 3). This means that the solar cells more efficiently convert light of lower energy photons. A further study taking PD2 as an example shows a clear dependence of the current increase on the dye load, see Figure S3. It is well-known that the dye load affects the maximum photon-to-electron generation and also the electron recombination loss at the $TiO_2$/electrolyte interface.

The mechanisms for any change occurring in a multi-component system, such as the DSSC devices, can be complicated. Therefore, we employed an approach based on selective exclusion of components in the normal electrolyte for


DOI: 10.1021/acsami.8b06897
ACS Appl. Mater. Interfaces 2018, 10, 26241−26247

**Table 1. Photovoltaic Parameters for DSSCs[a] Sensitized by PD2 and LEG1, Respectively, before and after 125 h of Light Exposure (*)**

| dyes | $V_{oc}$/mV | $J_{sc}$/mA cm$^{-2}$ | FF | $\eta^b$/% |
|---|---|---|---|---|
| LEG1 | 0.74 ± 0.01 | 8.3 ± 0.2 | 0.62 ± 0.01 | 3.8 ± 0.1 |
| LEG1* | 0.74 ± 0.02 | 12.9 ± 0.2 | 0.63 ± 0.01 | 6.0 ± 0.1 |
| PD2 | 0.72 ± 0.03 | 6.3 ± 0.3 | 0.68 ± 0.01 | 3.0 ± 0.1 |
| PD2* | 0.74 ± 0.02 | 11.4 ± 0.5 | 0.69 ± 0.03 | 5.8 ± 0.1 |

[a]DSSCs were assembled with the normal electrolyte consisting of 0.3 M/0.15 M Co(bpy)$_3^{2+/3+}$ and 0.2 M TBP in acetonitrile. [b]Efficiencies were recorded under full sun irradiation (AM 1.5G, ~100 mW/cm$^2$).

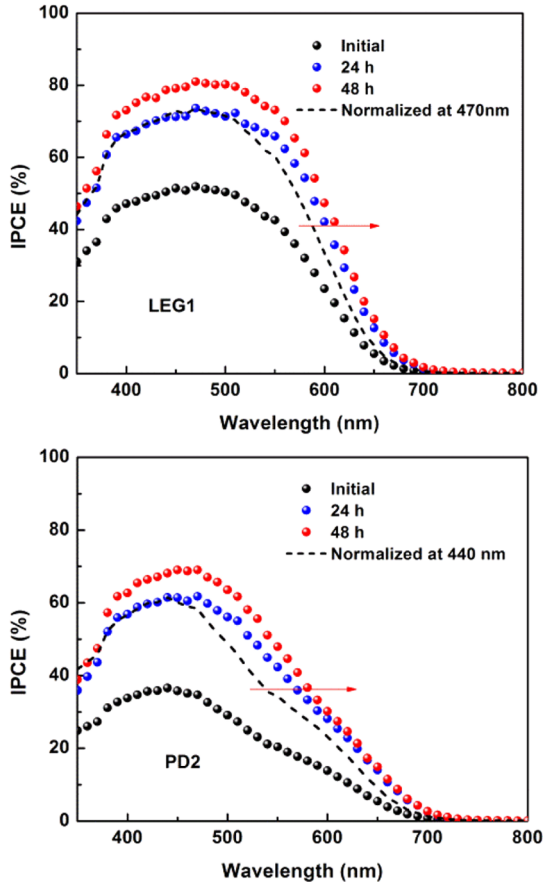


**Figure 3.** Evolution of IPCE spectra with time for DSSCs sensitized by the dyes LEG1 (top) and PD2 (bottom) during light exposure. Dashed IPCE spectra are given for the initial DSSC IPCE normalized to the values of the corresponding DSSCs aged 24 h; 470 nm (LEG1) and 440 nm (PD2), respectively.

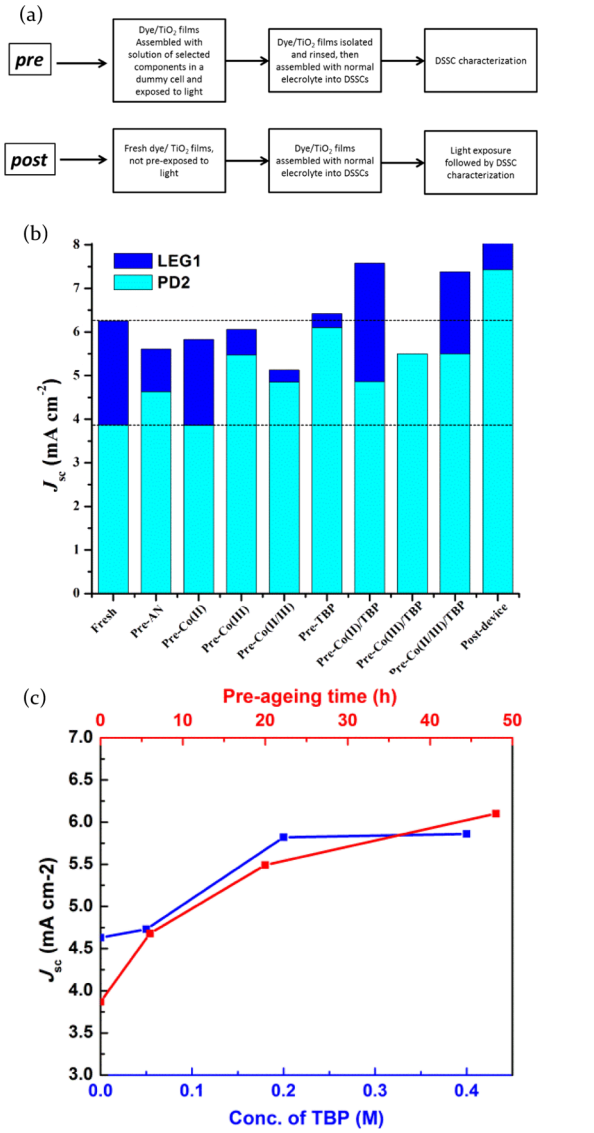


**Figure 4.** (a) Schematic illustration of the ***pre*** and ***post*** strategies used for light soaking treatment of DSSCs; (b) integrated current density based on IPCE spectra for LEG1- and PD2-sensitized DSSCs without treatment (**Fresh**) and after ***pre***-treatment varying the dummy electrolyte components as labeled, and ***post***-treatment, respectively for 48 h; (c) integrated $J_{sc}$ of PD2-sensitized DSSCs by ***pre***-treated in the dummy electrolytes containing TBP only varying the TBP concentration (48 h was fixed; blue) and treatment time (0.2 M TBP was fixed; red). The 0 concentration data points represent 0 M TBP for 48 h (blue) and 0.2 M TBP without light soaking (red).

working cells, including the solvent: acetonitrile (AN), the redox couple: Co(bpy)$_3^{2+/3+}$ [Co(II)/Co(III)], and the additive TBP to identify the origin for the performance improvement from the electrolyte perspective. The concentrations of these components in the dummy electrolytes were the same as for the normal electrolyte unless otherwise stated. Here, three different light soaking treatments based on the entire devices or the dye/$TiO_2$ electrodes were employed throughout the article: (1) ***Fresh***: no treatment and characterized immediately after fabricated; (2) ***Pre*** and (3) ***Post*** as schematically illustrated in Figure 4a. According to a ***pre*** strategy, the dye-sensitized $TiO_2$ film or electrode was pretreated under light exposure in a dummy cell with the dummy electrolyte containing certain component(s) as noted and then isolated. The ***pre***-treated electrode was re-assembled with the normal electrolyte and the counter electrode as a ***pre***-treated device for performance evaluation. ***Post*** strategy is for normal DSSC devices exposed to light soaking after being fabricated and were compared with ***Fresh*** and ***pre***-treated ones. Theoretically, the dye/$TiO_2$ film in ***post***-treated device is supposed to be the same with that after being ***pre***-treated in the normal electrolyte, that is, the sample of **Pre-E**. However, one should bear in mind that a certain amount of dye loss could be caused by isolating ***pre***-treated dye film from the dummy cell due to the presence of a base (e.g., TBP) and an oxidant [e.g., Co(III)] in the electrolyte composition. Dye loss could lead to a slight decrease in the photocurrent. Therefore, the character-


DOI: 10.1021/acsami.8b06897
ACS Appl. Mater. Interfaces 2018, 10, 26241−26247

ization results of PD2-sensitized solar cells based on the ***pre***-treatment strategy are more representative than LEG1 because the stronger $TiO_2$ binding of the former dye reduces the interference of dye loss. As shown in Figure 4b, for both dyes, the ***post*** strategy shows the largest increase in the current, whereas the main contribution to the current improvement for the ***pre*** strategy can be attributed to TBP present in the dummy electrolyte. One reason for the lower $J_{sc}$ of ***pre*-TBP** than the ***post*-device** could be dye loss or surface damage during the pre-treatment. The same TBP correlation applies to LEG1-based solar cells only in the co-presence of Co(II). This is logical because dissolved dye molecules are more prone to oxidative degradation than the adsorbed ones, and the presence of Co(II) can exercise a stabilizing effect for LEG1 which is more easily desorbed because of the presence of TBP. Consistently, the crucial effect of TBP was also observed on the increase in the IPCE spectra below ~600 nm, as shown in Figure S4a,b. Compared with the over 100% increase in the IPCE ranging from 500 to 600 nm for devices based on the ***post*** strategy, the presence of TBP only in ***pre*** strategy contributes almost 70%. Figure 4c and Table S1 shows that the improvement of the device photocurrent under light exposure is increased by increasing the concentration of TBP in the dummy electrolyte for ***pre***-treatment, which levels off at 0.2 M, and by increasing the treatment time under light soaking. The concentration and time dependences confirm the role of TBP in the performance improvement and could be interpreted as more access of TBP to the dye/$TiO_2$ interface. IPCE spectra show a larger increase below 600 nm, while at longer wavelength instead a decrease (Figure S4c). The latter effect could be related to basic TBP causing dye loss.

Figure S5 shows the photoinduced absorption (PIA) spectra of DSSCs based on PD2 and LEG1, respectively, before and after light exposure, corresponding to the absorption difference of the samples between the ground state and the steady state after square-wave light excitation. The bleach peaks at 500 nm for PD2 and 550 nm for LEG1 are known to be caused by a Stark effect on the dye ground state as a result of the local electric field at the $TiO_2$/dye/electrolyte interface generated by the injected electrons. It can be noted that the bleach intensity is lower for both LEG1- and PD2-based DSSCs after light soaking, and the spectra are red-shifted by ~20 nm. The changes indicate more mobile electrons in the $TiO_2$, faster rearrangement of the environment around the dye in response to charge changes, or more efficient dye regeneration. The electron-transfer kinetics were further investigated based on three strongly correlated interfaces and corresponding processes: (1) at dye/$TiO_2$ interface electron injection from the excited state of the dye into the $TiO_2$ conduction band or recombination; (2) dye regeneration at the dye/electrolyte interface; and (3) at $TiO_2$/electrolyte interface recombination from the $TiO_2$ conduction band and trap states to electrolyte oxidants.

The most significant change was observed in the electron injection kinetics studied by femtosecond transient absorption spectroscopy, as depicted in Figure 5 and Table 2. By using a mono-exponential model of the injected electron absorption increase, it can be deduced that the electron injection time ($\tau_{inj,1}$) of PD2 decreases from ca. 700 (**Fresh**) to 200 fs by prolonging the ***pre***-strategy treatment in TBP solution up to 15 h, or in TBP-containing normal electrolytes for longer time (50 h); that is, the femtosecond-scale injection becomes faster. Here, the dye/$TiO_2$ film after pre-treatment in the normal

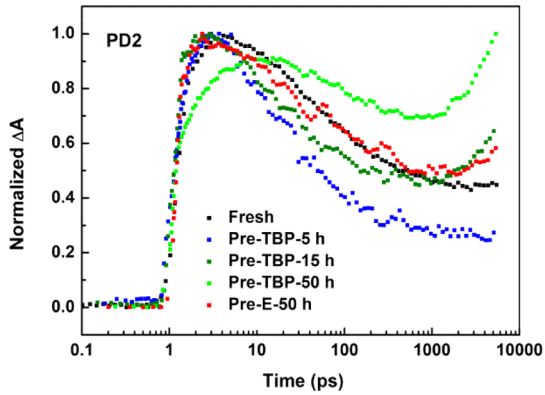


**Figure 5.** Normalized kinetic curves ($\Delta A$ at ~5000 nm) of electron injection/recombination processes for PD2-sensitized $TiO_2$ films after being ***pre***-treated in a 0.2 M TBP/AN solution (**Pre-TBP**) and the normal electrolyte (**Pre-E**) for different time.

**Table 2. Electron-Transfer Kinetic Halftimes at the PD2/$TiO_2$ Interface for Fresh and *Pre*-Treated Samples in TBP Only (Pre-TBP) and the Normal Electrolyte (Pre-E) for Different Time**[a]

| | electron injection | | electron recombination | | |
|---|---|---|---|---|---|
| samples | $\tau_{inj,1}$/ps | $\tau_{inj,2}$ | $\tau_{rec,1}$/ps | $\tau_{rec,2}$/ps | $\tau_{rec,long}$ (>5 ns) |
| **Fresh** | 0.7 | | 35 (33) | 300 (22) | $\tau_3$ (45) |
| **Pre-TBP-5 h** | 0.5 | | 13 (49) | 135 (27) | $\tau_3$ (24) |
| **Pre-TBP-15 h** | 0.2 | ns | 18 (9) | 230 (4) | $\tau_3$ (87) |
| **Pre-TBP-50 h** | 1.5 | ns | 180 (3) | | $\tau_3$ (97) |
| **Pre-E-50 h** | 0.4 | ns | 16 (25) | 170 (25) | $\tau_3$ (50) |

[a]Values in the brackets indicate the contribution (%) of the lifetime parameter in the model used.

electrolyte, that is, the sample of **Pre-E**, in principle should present similar kinetics as in the post-treated devices. Unexpectedly, a new injection component with a much slower kinetics ($\tau_{inj,2}$, ns timescale) follows by when increasing the ***pre***-treatment time to more than 15 h and interferes the recombination process of the similar timescale ($\tau_{rec,1}$, $\tau_{rec,2}$, below 5 ns, the maximum time range that could be determined in the experiments). The kinetics of the recombination corresponding to the slow injection could be obtained by multi-exponential modeling with one more parameter: $\tau_{rec,long}$, >5 ns and likely extending to milliseconds. $\tau_{inj,2}$ and $\tau_{rec,long}$ cannot be properly determined in this work as it is beyond the detection limit. However, it can be observed that the fraction of the slow injection/recombination components increases with the treatment time. This causes that up to 50 h ***pre***-treatment in TBP only, electrons involved in the fast injection pathway decrease. As a result, a much longer lifetime of injected electrons and more efficient electron collection is expected for the ***pre***-treated devices compared with fresh ones. A similar effect was also observed in LEG1-based systems; see Figure S6 and Table S2. The transient open-circuit voltage decay shows the kinetics of $TiO_2$/electrolyte interfacial recombination to be in the millisecond timescale. In coherence with the results above, ***pre***-treatment in the presence of TBP renders a longer electron lifetime ($\tau_n$) in $TiO_2$, see Figures 6a and S7. In addition, the improvement seems to increase with higher concentrations of TBP and longer treatment time. This explains the photocurrent increase, showing the same depend-


DOI: 10.1021/acsami.8b06897
ACS Appl. Mater. Interfaces 2018, 10, 26241−26247

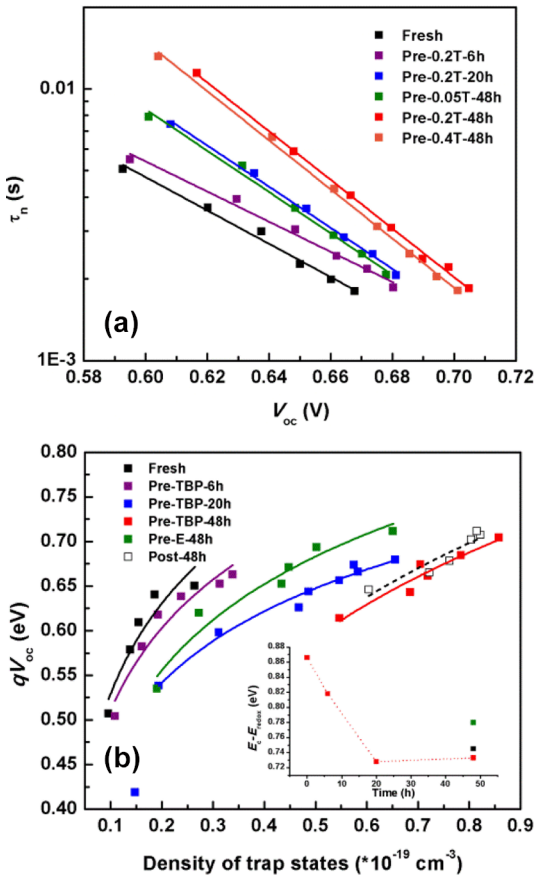


**Figure 6.** (a) Electron lifetime ($\tau_n$) in $TiO_2$ of PD2-based DSSCs treated according to ***pre*** strategy as a function of the TBP concentration in the electrolyte from 0.05 to 0.4 M (for instance, labeled as **0.05T** for 0.05 M TBP) and of the treatment time from 6 to 48 h, as labeled; (b) trap state distribution in $TiO_2$ of PD2-based DSSCs containing an nontreated dyed film (**Fresh**) and treated according to ***pre*** strategy (**Pre**) in 0.2 M TBP solution for different times, as labeled, and in the normal electrolyte for 48 h and DSSCs after light exposure (**Post**) for 48 h. Plots in (a) are linearly modeled with respect to the logarithmic value of $\tau_n$ and in (b) were modeled using exponential functions,[25] providing the parameter $E_c - E_{redox}$, correspondingly shown in the inset figure.

ency in Figure 4c. The absorption decay of dye cations was monitored to investigate the kinetics of dye regeneration by the TBP-containing cobalt electrolyte. As shown in Figure S8 and Table S3, the observed kinetics increase by a factor of 2 for both PD2 and LEG1 after the systems have been exposed to light. It has been suggested that the regeneration kinetics depends on the driving force for regeneration, that is, the gap between the energy levels of the dye highest occupied molecular orbital (HOMO) and the redox potential of the electrolyte, and concentrations of the redox system components used as well. It has been proved in our previous work that the redox potential shows small changes to extended light exposure. All these results suggest a shift in the dye HOMO energy level and/or a rearrangement of the dye molecules on the $TiO_2$ surface.

The energy state distribution at the $TiO_2$ surface was estimated by charge extraction measurements; see Figures 6b and S9b. The conduction band edge of $TiO_2$ ($E_c$) was observed to shift by ~0.15 eV toward more positive potentials when increasing the ***pre***-treatment time with TBP, regardless of the negligible change in the redox potential of the electrolyte ($E_{redox}$). The same effect was also observed in the ***pre*** treatments based on the normal electrolyte and the ***post*** treatment of the devices. It has been well-known that $TiO_2$ $E_c$ shifts are caused by surface adsorbed species including dipoles and charges; in our case, the shifts are caused by electronic coupling between $E_c$ and the low-lying unoccupied molecular orbitals (LUMO) of the attached dyes.[26] More efficient electron transfer, as concluded above, points out two other possible reasons for the observed downshift of the $E_c$: (1) a decrease in the surface dipole effect normal to the surface and (2) a change in the electronic coupling to lower energy unoccupied orbitals of the dye. Valence-level photoelectron spectroscopic investigations including metastable-induced electron spectroscopy/ultraviolet photoelectron spectroscopy (MIES/UPS) were performed to trace the changes in density of states at the dye/$TiO_2$ interface. The work function, which is associated with the onset of the UP spectrum, is provided in Table S4. It can be observed that for both types of dyes, the work function of the dye/$TiO_2$ film increases after the ***pre*** treatment in the presence of TBP. Furthermore, the spectra as a whole of both UPS and MIES shift (around 0.3 eV) toward lower electron binding energies with respect to the vacuum level, see Figures 7 and S10. This means that the energy level

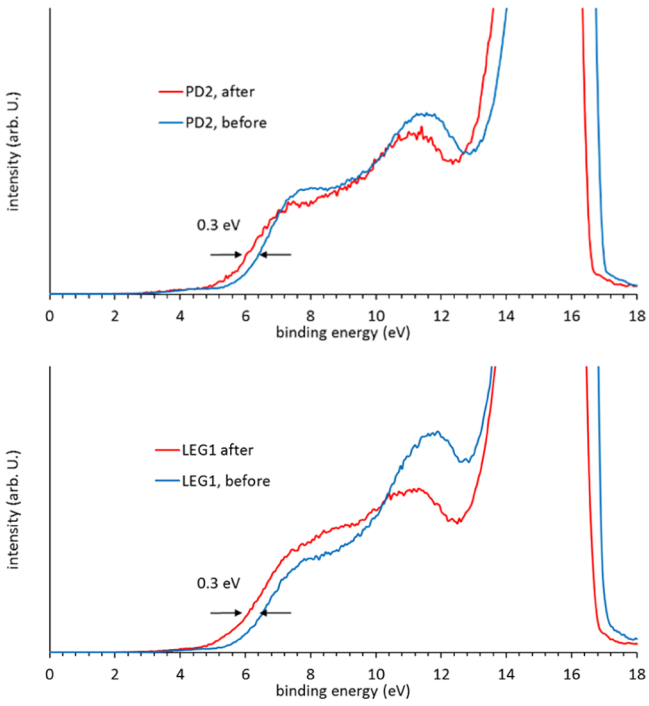


**Figure 7.** MIE spectra of PD2/$TiO_2$ (top) and LEG1/$TiO_2$ (bottom) films before (blue) and after (red) exposure to a 0.2 M TBP AN solution and light. A shift of about 0.3 eV applies for both spectra.

of the HOMO of the dye is up-shifted, which is caused by a change in the dipole interaction between the dye layer and the $TiO_2$. A change in dipole interaction can result from re-orientation or desorption of the dye molecules, or by the adsorption or desorption of other species. We can presume that some changes due to the ***pre*** treatment, occurring at the dye/$TiO_2$ interface, lead to either a re-alignment of the interfacial energy levels influencing the charge-transfer pattern,[27] or vice versa (more efficient charge transfer contributing to the shifts of both dye and $TiO_2$ energy levels).


DOI: 10.1021/acsami.8b06897
ACS Appl. Mater. Interfaces 2018, 10, 26241−26247

Additionally, the absorption spectra of the dye/$TiO_2$ film shows little shift after light soaking (Figure S11), which indicates that dye energy of the lowest unoccupied molecular orbital (LUMO) is up-shifted around 0.3 eV as well. For these reasons, and including the shift of 0.15 eV in the $TiO_2$ conduction band, the driving force for electron injection is indicated to increase by ~0.45 eV. This means that the electrons also exited at longer wavelengths will experience lower barriers for injection into the $TiO_2$ substrate. This is highly consistent with the increase in the IPCE in the red region as mentioned above. Coupling to lower energy levels could lead to a new injection pathway, which also agrees with the observed new slow injection component after light treatment.

The shift of energy levels indicates a change in the electronic coupling at the dye/$TiO_2$ interface, which could result from a change in the binding mode or dye assembly on the surface. By inspecting the molecular orbital contribution to the MIE spectra of the dye/$TiO_2$ films in Figure S12 and evaluating the intensity variation of each peak after the ***pre*** treatment in Figure S12 and Table S5, peaks related to the bithiophene linker show a significant decrease in intensity while the peaks of the alkyl and benzene donor group increase in intensity. These spectral changes are more noticeable in the case of LEG1, which is more susceptible to the presence of the TBP-containing electrolyte. This result indicates that top-layered dye molecules are re-oriented after the ***pre*** treatment, with the bottom $TiO_2$ as reference. An H-type (head to head) aggregation has been suggested by the blue shift in the spectra of the dye film with increasing dye load, as shown in Figure S13. From the UV−vis spectra alone, it cannot be deduced if this aggregation is in the form of multilayer aggregates or in the form of a single surface layer (monolayer); both offering the possibility of close proximity between the dye molecules in a parallel fashion. As recently shown, the model organic dye L0Br assembles in a mixed multilayer/monolayer configuration, with a preference for the latter.[28] The dyes PD2 and LEG1 with more extended $\pi$-systems are expected to promote aggregation, possibly inducing a preference for multilayer aggregation. After re-orientation, top-layered dye molecules either bonded to $TiO_2$ as a monolayer or nonadsorbed as J-type aggregates, contribute to increasing the dipole moment on the surface and more direct routes for electron injection into the $TiO_2$ substrate, which would account for the change in the injection kinetics as mentioned above.

The crucial role of TBP in the light-induced change at the dye/$TiO_2$ interface could be attributed to its basic properties. The adsorption process of dye onto the $TiO_2$ surface may be regarded as an acid/base reaction, which is known to be strongly affected by the acidity of the liquid environment. Therefore, the arrangement of dye on the surface, which has been demonstrated to be a dynamic process, is also influenced by the presence of acid/basic additives in the electrolyte, such as TBP in this work. The trigger for the change, as suggested by this work, could be light or thermal stress. One effect of the basic additive is dye desorption. However, the desorption of the dye, which can be achieved simply by using a stronger base, cannot provide the same efficiency improvement as observed from the ***pre*** treatment in TBP solution, see Table S6. It is readily observed that the adsorption isotherms of PD2 and LEG1 in Figure S14 are correlated with their device efficiency evolution shown in Figure 2. By contrast, much higher concentration of PD2 in solution is required. The differences in adsorption isotherms reflect the differences in both surface adsorption strength and solvent interaction strength. It could be thus derived that the difference in the efficiency improvement between PD2 and LEG1 results from their differences in both surface adsorption and interaction with TBP. The TBP-involved interaction changes the adsorption/desorption equilibrium of the dye, therefore facilitating a re-arrangement of dyes on the $TiO_2$ surface under light exposure.

In conclusion, we have shown an effective strategy to investigate a phenomenon of performance improvement of DSSCs during light soaking. This work, based on two similar organic dyes differing only in anchoring properties, identifies the crucial effect of the electrolyte and, more specifically TBP additives, on the dynamics at the $TiO_2$/dye/electrolyte interface under light exposure. The effects are manifested by the change in interfacial energetics, charge-transfer mode, and kinetics, which suggest a dye re-arrangement on the electrode surface. Although the details still need to be further clarified, the work certainly highlights that the electrolytes are far from innocent spectators under device operation, and that they need to be optimized for the sake of both initial efficiency and long-term stability of the devices. Because TBP is a widely used electrolyte additive for DSSCs and other electrochemical systems, this work will provide a platform for future research on the surface dynamics in this area. The results from this work also emphasize the need for a better understanding of the fundamental in situ/in operando chemistry in such devices.

## ■ ASSOCIATED CONTENT

### Supporting Information

The Supporting Information is available free of charge on the ACS Publications website at DOI: 10.1021/acsami.8b06897.

Experimental details, additional figures and tables including solar cell performance variation, transient absorption kinetic traces and fitting parameters, toolbox, and UV−vis and PIA spectroscopy results (PDF)

## ■ AUTHOR INFORMATION


### Corresponding Author

*E-mail: Lakloo@kth.se and Larsa@kth.se.

### ORCID

James M. Gardner: 0000-0002-4782-4969
Gunther Andersson: 0000-0001-5742-3037
Lars Kloo: 0000-0002-0168-2942


### Author Contributions

The manuscript was written through contributions of all authors. All authors have given approval to the final version of the manuscript.

### Notes

The authors declare no competing financial interest.

## ■ ACKNOWLEDGMENTS

We gratefully acknowledge the Swedish Research Council, the Swedish Energy Agency as well as the China Scholarship Council (CSC) for the financial support.

## ■ REFERENCES

(1) Mathew, S.; Yella, A.; Gao, P.; Humphry-Baker, R.; Curchod, B. F. E.; Ashari-Astani, N.; Tavernelli, I.; Rothlisberger, U.; Nazeeruddin, M. K.; Grätzel, M. Dye-sensitized Solar Cells with 13% Efficiency



DOI: 10.1021/acsami.8b06897
ACS Appl. Mater. Interfaces 2018, 10, 26241−26247

Achieved Through the Molecular Engineering of Porphyrin Sensitizers. *Nat. Chem.* **2014**, *6*, 242−247.
(2) Hong, Y.; Liao, J.-Y.; Cao, D.; Zang, X.; Kuang, D.-B.; Wang, L.; Meier, H.; Su, C.-Y. Organic Dye Bearing Asymmetric Double Donor-π-Acceptor Chains for Dye-Sensitized Solar Cells. *J. Org. Chem.* **2011**, *76*, 8015−8021.
(3) Haid, S.; Marszalek, M.; Mishra, A.; Wielopolski, M.; Teuscher, J.; Moser, J.-E.; Humphry-Baker, R.; Zakeeruddin, S. M.; Grätzel, M.; Bäuerle, P. Significant Improvement of Dye-Sensitized Solar Cell Performance by Small Structural Modification in π-Conjugated Donor-Acceptor Dyes. *Adv. Funct. Mater.* **2012**, *22*, 1291−1302.
(4) Yang, J.; Ganesan, P.; Teuscher, J.; Moehl, T.; Kim, Y. J.; Yi, C.; Comte, P.; Pei, K.; Holcombe, T. W.; Nazeeruddin, M. K.; Hua, J.; Zakeeruddin, S. M.; Tian, H.; Grätzel, M. Influence of the Donor Size in D−π-A Organic Dyes for Dye-Sensitized Solar Cells. *J. Am. Chem. Soc.* **2014**, *136*, 5722−5730.
(5) Duan, T.; Fan, K.; Li, K.; Cao, W.; Zhong, C.; Chen, X.; Peng, T.; Qin, J. Design of organic dyes for dye-sensitized solar cells: Extending π-conjugation backbone via 'Click' reaction to improve photovoltaic performances. *Dyes Pigm.* **2015**, *117*, 108−115.
(6) Wang, X.-F.; Kitao, O.; Zhou, H.; Tamiaki, H.; Sasaki, S.-i. Extension of π-conjugation length along the Qy axis of a chlorophyll a derivative for efficient dye-sensitized solar cells. *Chem. Commun.* **2009**, 1523−1525.
(7) Wang, X.-F.; Fujii, R.; Ito, S.; Koyama, Y.; Yamano, Y.; Ito, M.; Kitamura, T.; Yanagida, S. Dye-sensitized Solar Cells Using Retinoic Acid and Carotenoic Acids: Dependence of Performance on the Conjugation Length and the Dye Concentration. *Chem. Phys. Lett.* **2005**, *416*, 1−6.
(8) Hahlin, M.; Johansson, E. M. J.; Plogmaker, S.; Odelius, M.; Hagberg, D. P.; Sun, L.; Siegbahn, H.; Rensmo, H. Electronic and Molecular Structures of Organic Dye/TiO2 Interfaces for Solar Cell Applications: a Core Level Photoelectron Spectroscopy Study. *Phys. Chem. Chem. Phys.* **2010**, *12*, 1507−1517.
(9) Buhbut, S.; Clifford, J. N.; Kosa, M.; Anderson, A. Y.; Shalom, M.; Major, D. T.; Palomares, E.; Zaban, A. Controlling Dye Aggregation, Injection Energetics and Catalytic Recombination in Organic Sensitizer Based Dye Cells Using a Single Electrolyte Additive. *Energy Environ. Sci.* **2013**, *6*, 3046−3053.
(10) Cho, C.-P.; Chu, C.-C.; Chen, W.-T.; Huang, T.-C.; Tao, Y.-T. Molecular Modification on Dye-sensitized Solar Cells by Phosphonate Self-assembled Monolayers. *J. Mater. Chem.* **2012**, *22*, 2915−2921.
(11) Rühle, S.; Greenshtein, M.; Chen, S.-G.; Merson, A.; Pizem, H.; Sukenik, C. S.; Cahen, D.; Zaban, A. Molecular Adjustment of the Electronic Properties of Nanoporous Electrodes in Dye-Sensitized Solar Cells. *J. Phys. Chem. B* **2005**, *109*, 18907−18913.
(12) Kazes, M.; Buhbut, S.; Itzhakov, S.; Lahad, O.; Zaban, A.; Oron, D. Photophysics of Voltage Increase by Photoinduced Dipole Layers in Sensitized Solar Cells. *J. Phys. Chem. Lett.* **2014**, *5*, 2717−2722.
(13) Yang, X.; Zhang, S.; Zhang, K.; Liu, J.; Qin, C.; Chen, H.; Islam, A.; Han, L. Coordinated Shifts of Interfacial Energy Levels: Insight into Electron Injection in Highly Efficient Dye-sensitized Solar Cells. *Energy Environ. Sci.* **2013**, *6*, 3637−3645.
(14) Pandey, S. S.; Lee, K.-Y.; Hayat, A.; Ogomi, Y.; Hayase, S. Investigating the Role of Dye Dipole on Open Circuit Voltage in Solid-State Dye-Sensitized Solar Cells. *Jpn. J. Appl. Phys.* **2011**, *50*, 06GF08.
(15) Agrawal, S.; Leijtens, T.; Ronca, E.; Pastore, M.; Snaith, H.; De Angelis, F. Modeling the Effect of Ionic Additives on the Optical and Electronic Properties of a Dye-sensitized TiO2 Heterointerface: Absorption, Charge Injection and Aggregation. *J. Mater. Chem. A* **2013**, *1*, 14675−14685.
(16) Oscarsson, J.; Hahlin, M.; Johansson, E. M. J.; Eriksson, S. K.; Lindblad, R.; Eriksson, A. I. K.; Zia, A.; Siegbahn, H.; Rensmo, H. Coadsorption of Dye Molecules at TiO2 Surfaces: A Photoelectron Spectroscopy Study. *J. Phys. Chem. C* **2016**, *120*, 12484−12494.
(17) Harima, Y.; Kawabuchi, K.; Kajihara, S.; Ishii, A.; Ooyama, Y.; Takeda, K. Improvement of Photovoltages in Organic Dye-sensitized Solar Cells by Li Intercalation in Particulate TiO2 Electrodes. *Appl. Phys. Lett.* **2007**, *90*, 103517.
(18) Ishii, H.; Sugiyama, K.; Ito, E.; Seki, K. Energy Level Alignment and Interfacial Electronic Structures at Organic/Metal and Organic/Organic Interfaces. *Adv. Mater.* **1999**, *11*, 605−625.
(19) Ford, W. E.; Gao, D.; Knorr, N.; Wirtz, R.; Scholz, F.; Karipidou, Z.; Ogasawara, K.; Rosselli, S.; Rodin, V.; Nelles, G.; von Wrochem, F. Organic Dipole Layers for Ultralow Work Function Electrodes. *ACS Nano* **2014**, *8*, 9173−9180.
(20) Zietz, B.; Gabrielsson, E.; Johansson, V.; El-Zohry, A. M.; Sun, L.; Kloo, L. Photoisomerization of the Cyanoacrylic Acid Acceptor Group - a Potential Problem for Organic Dyes in Solar Cells. *Phys. Chem. Chem. Phys.* **2014**, *16*, 2251−2255.
(21) Fredin, K.; Anderson, K. F.; Duffy, N. W.; Wilson, G. J.; Fell, C. J.; Hagberg, D. P.; Sun, L.; Bach, U.; Lindquist, S.-E. Effect on Cell Efficiency following Thermal Degradation of Dye-Sensitized Mesoporous Electrodes Using N719 and D5 Sensitizers. *J. Phys. Chem. C* **2009**, *113*, 18902−18906.
(22) Yang, L.; Xu, B.; Bi, D.; Tian, H.; Boschloo, G.; Sun, L.; Hagfeldt, A.; Johansson, E. M. J. Initial Light Soaking Treatment Enables Hole Transport Material to Outperform Spiro-OMeTAD in Solid-State Dye-Sensitized Solar Cells. *J. Am. Chem. Soc.* **2013**, *135*, 7378−7385.
(23) Tiwana, P.; Docampo, P.; Johnston, M. B.; Herz, L. M.; Snaith, H. J. The origin of an efficiency improving "light soaking" effect in SnO2 based solid-state dye-sensitized solar cells. *Energy Environ. Sci.* **2012**, *5*, 9566−9573.
(24) Gabrielsson, E.; Tian, H.; Eriksson, S. K.; Gao, J.; Chen, H.; Li, F.; Oscarsson, J.; Sun, J.; Rensmo, H.; Kloo, L.; Hagfeldt, A.; Sun, L. Dipicolinic acid: a strong anchoring group with tunable redox and spectral behavior for stable dye-sensitized solar cells. *Chem. Commun.* **2015**, *51*, 3858−3861.
(25) Gao, J.; Yang, W.; Pazoki, M.; Boschloo, G.; Kloo, L. Cation-Dependent Photostability of Co(II/III)-Mediated Dye-Sensitized Solar Cells. *J. Phys. Chem. C* **2015**, *119*, 24704−24713.
(26) Ronca, E.; Pastore, M.; Belpassi, L.; Tarantelli, F.; De Angelis, F. Influence of the dye molecular structure on the TiO2conduction band in dye-sensitized solar cells: disentangling charge transfer and electrostatic effects. *Energy Environ. Sci.* **2013**, *6*, 183−193.
(27) Zheng, J.; Zhang, K.; Fang, Y.; Zuo, Y.; Duan, Y.; Zhuo, Z.; Chen, X.; Yang, W.; Lin, Y.; Wong, M. S.; Pan, F. How to Optimize the Interface between Photosensitizers and TiO2 Nanocrystals with Molecular Engineering to Enhance Performances of Dye-Sensitized Solar Cells? *ACS Appl. Mater. Interfaces* **2015**, *7*, 25341−25351.
(28) Liu, P.; Johansson, V.; Trilaksana, H.; Rosdahl, J.; Andersson, G. G.; Kloo, L. EXAFS, ab Initio Molecular Dynamics, and NICIS Spectroscopy Studies on an Organic Dye Model at the Dye-Sensitized Solar Cell Photoelectrode Interface. *ACS Appl. Mater. Interfaces* **2017**, *9*, 19773−19779.


DOI: 10.1021/acsami.8b06897
*ACS Appl. Mater. Interfaces* 2018, 10, 26241−26247